



HAL
open science

Effect of variability of hemp shiv on the setting of lime hemp concrete

Lepeng Wang, H el ene Lenormand, Hafida Zmamou, Nathalie Leblanc

► **To cite this version:**

Lepeng Wang, H el ene Lenormand, Hafida Zmamou, Nathalie Leblanc. Effect of variability of hemp shiv on the setting of lime hemp concrete. *Industrial Crops and Products*, 2021, 171, pp.113915. 10.1016/j.indcrop.2021.113915 . hal-03383074

HAL Id: hal-03383074

<https://hal.science/hal-03383074>

Submitted on 22 Aug 2023

HAL is a multi-disciplinary open access archive for the deposit and dissemination of scientific research documents, whether they are published or not. The documents may come from teaching and research institutions in France or abroad, or from public or private research centers.

L'archive ouverte pluridisciplinaire **HAL**, est destin ee au d ep ot et  a la diffusion de documents scientifiques de niveau recherche, publi es ou non,  emanant des  tablissements d'enseignement et de recherche fran ais ou  trangers, des laboratoires publics ou priv es.



Distributed under a Creative Commons Attribution - NonCommercial 4.0 International License

1 Effect of variability of hemp shiv on the setting of lime hemp concrete

2 Lepeng Wang¹, H el ene Lenormand¹, Hafida Zmamou^{1*}, Nathalie Leblanc¹

3 ¹UniLaSalle, Univ. Artois, ULR7519 - Transformations & Agro-ressources, Normandie Universit e, 3 rue du Tronquet,

4 F-76130 Mont-Saint-Aignan, France.

5 *Corresponding Author: Hafida Zmamou. Email: hafida.zmamou@unilasalle.fr.

6

7 **Abstract**

8 Lime hemp concrete (LHC) is one of the most environmentally friendly alternatives to traditional
9 building materials, which is normally used as an insulation material. The lime hemp concrete is
10 made up of hemp shiv and aerial (or hydraulic) lime and has the ability to offer better thermal and
11 acoustic performances. However, it is reported that the shiv/matrix reaction does not always meet
12 the expectations, thus the properties of hemp concrete may be affected by certain characteristics,
13 such as origin, retting time, harvest time, etc. of the used hemp. During this work, the authors
14 have studied the influence of variability of hemp shiv on the setting of LHC. The results depicted
15 that the soluble components (e.g., organic acids, simple sugars, etc.) from hemp shiv had a
16 significant impact on the setting and hardening of mortars. This study also proved that hemp
17 containing more soluble components tends to involve a longer setting time and hinders long-term
18 carbonation reaction of binders. Furthermore, the experimental results also showed that water
19 treatment can effectively remove these soluble agents from hemp shiv and improve the
20 compatibility between shiv and binder in the composite.

21 **Keywords:** Hemp shiv; setting time; carbonation reaction; retting; hemp shiv leachate

22 **1. Introduction**

23 The **production of cement** contributes about 5-7% to global CO₂ emissions and 2% to overall
24 energy consumption (Benhelal et al., 2013; Worrell et al., 2001), so it is necessary to develop
25 cement substitutes having low environmental impact. The binder such as cement is considered to
26 be the main contributor to the environmental impact as demonstrated by the life cycle assessment
27 (Prétot et al., 2014). Therefore, alternative binder materials (e.g., geopolymers, lime, pozzolans,
28 etc.) are attracting increasing interests in research and development during the past decades. At
29 the same time, recent investigations indicated that plant aggregates have interesting
30 environmental and economic benefits (Sanjay et al., 2018; Sáez-Perez et al., 2020), and they
31 could be used to replace conventional aggregates. Hemp shiv is the byproduct of hemp fibers
32 production, which is the most widely used plant aggregate of lightweight concretes. Hemp shiv is
33 derived from woody core (composed of xylem and pith), whereas the bark (composed of
34 epidermis, bast fibers and cambium) is considered as principal source of hemp fibers (Sáez-Perez
35 et al., 2020). **LHC**, was reported to possess excellent thermal and acoustic performances e.g.,
36 thermal isolation, sound absorption, soundproofing, etc. (Elfordy et al., 2008) , which could be
37 effectively employed as an insulation material, coating, and even bricks. Owing to the carbon
38 storage effect of lime carbonation and hemp cultivation, **LHC** has a weaker ecological impact
39 compared to traditional building materials (Ip and Miller, 2012; Hirst et al., 2010). Keeping in
40 view its excellent thermal insulation property, the application of LHC can reduce long-term
41 energy consumptions of the building.

42 Despite these advantages of hemp concrete, the wide-use of LHC is still limited due to certain
43 drawbacks. An essential disadvantage of LHC is **its** poor strength performance, thus limiting its
44 use as a load-bearing material (Tronet et al., 2016). The poor mechanical performance is mainly
45 triggered by the intrinsic mechanical properties of aggregates (hemp shiv). Another problem
46 which affects the application of LHC is the incompatibility that exists between hemp shiv and

47 binder (lime, cement), thus leading to a setting delay and a large variability of thermal and
48 acoustic properties. The previous works have illustrated that the various factors such as origin
49 (Diquélou et al., 2015), harvest time, field retting (Li et al., 2009) of hemp shiv, binder types
50 (Walker et al., 2014) can influence the compatibility. It was reported that thermal and chemical
51 treatments might enhance the compatibility between plant aggregates and the binder (Bilba et al.,
52 2003; Khazma et al., 2012; Sedan et al., 2008), but this will result in an increase in costs and
53 carbon emissions. It is therefore important to find an economic and ecological approach for the
54 treatment of hemp to meet the application needs of bio-aggregate based building materials.

55 Empirical observations indicate that "rotten" hemp shiv (or other byproducts of plant fibers
56 production) tend to have better aggregate/matrix interaction (i.e., shorter setting time and better
57 mechanical performance). Depending upon industrial requirements, a certain level of retting may
58 be required. Retting is a critical step in the production of fiber from plant material (Martin et al.,
59 2013). The most widely used method of retting is the field retting which requires the action of
60 micro-organisms and moisture on plants to dissolve or rot away the stem material surrounding the
61 fiber bundles. However, field retting is highly climate-dependent, and its mechanism has not yet
62 been completely understood by the researchers. It has been reported that as the retting time
63 increases, the color of the hemp fiber becomes darker and the tensile strength increases (Mazian
64 et al., 2018). Meijer et al. (1995) found that the degradation of pectin is the key process in retting
65 and can be used as a measure of the degree of retting. At the same time, the colorimeter,
66 thermogravimetric analysis (TGA), and FT-IR spectrum analyses were also reviewed to evaluate
67 the retting degree (Sedan et al., 2008; Martin et al., 2013). However, until now, no indicator or
68 method is sensitive enough to determine the variability of the degree of retting of hemp shiv
69 available in the market.

70 So, the current work focuses on the influence of hemp variability on the setting of the matrix.
71 Four samples of hemp shiv were analyzed for producing water leachate and the hemp shiv

72 through water treatment which were characterized and added to the lime binder. During this
73 process , setting time and the carbonation reaction of mortars have been monitored.

74 **2. Materials and methods**

75 **2.1 Raw materials**

76 Hemsps utilized in the present study were grown in France, and these were pulled and dew-retted
77 in the field during September. This process took 30 to 40 days as it was dependent on the climate
78 and experience of farmers. Due to the fact that field retting involves complex biochemical
79 reactions, and the retting degree is strongly affected by climatic conditions, the relation between
80 the retting process (i.e., retting time and retting method) and retting degree was not discussed
81 during our study. Four types of hemp shiv (i.e., B1-B4), with different localisation origins, were
82 included in current research and are presented in section 2.2. The choice of samples was made on
83 the basis of their color, whereas, the variability of shiv was analyzed and compared by the color,
84 leachate concentration, infrared spectrum analysis and biochemical composition.

85 The binder employed in this study was Tradical PF70 of Lhoist, an air lime pre-formulated
86 binder, which is widely used for the manufacture of hemp concrete blocks and insulation in
87 Europe. Tradical PF70 consists of 75 wt% hydrated lime, 15 wt% hydraulic binder and 10 wt% of
88 the pozzolanic material. The purpose of the hydraulic binder (e.g., Portland cement) is to improve
89 early age properties such as setting time and strength development, whilst the pozzolans can
90 reduce the use of cement (Walker and Pavía, 2014).

91 **2.2 Sample preparation and experimental methods**

92 The schematic presentation of the sample preparation process is shown in Fig. 1. Hemp shiv were
93 ground to 2 mm particles, then submerged in water for 24 hours (water treatment), under
94 mechanic agitation. After this water treatment, the shiv and leachate were separated by filter

95 paper having pore size of 10 μm . The shiv before (B) and after (C) water treatment are shown in
96 Fig. 2, which indicate that the 24 hours of water treatment had no significant effect on the color of
97 hemp shiv. Since the hemp shiv has a strong water absorption performance, after preliminary
98 tests, the water ratio was set to 1:20 to ensure that a sufficient and suitable concentration of the
99 leachate was obtained. It is worth noting that the weight of the leachate (D) in Fig. 2 was the
100 theoretical value, the real weight which was obtained during the analysis was less than 201g due
101 to filtration and drying.

102 *Location of Figure 1*

103 *Location of Figure 2*

104 **2.2.1 pH and conductivity analysis of leachate**

105 The leachate (D1-D4) of hemp shiv were analyzed by pH-meter and conductivity using a
106 THERMO Orion Star A11 equipment.

107 **2.2.2 Infrared spectrum analysis of hemp shiv**

108 Fourier Transform Infrared Spectrometry (FT-IR) in transmission mode with a Nicolet iS10 FT-
109 IR spectrometer was used to analyze solid samples. The transmission spectra were recorded with
110 a resolution of 2 cm^{-1} and a wavenumber range of 4000-650 cm^{-1} .

111 **2.2.3 Spectrocolorimetry of hemp shiv**

112 Color determination of hemp shiv powders was carried out using a spectrophotometer (CM-
113 2300d, Konika Minolta, Japan). Color was measured by means of CIELab coordinates (ISO
114 11664-4:2008): L^* (whiteness ($L^*=0$) or brightness ($L^*=100$)), a^* (redness ($a^*>0$) or greenness
115 ($a^*<0$)) and b^* (yellowness ($b^*>0$) or blueness ($b^*<0$)). Hemp shiv powders were obtained after
116 milling of hemp shiv (previously dried until constant weight at 40°C) employing a micro impact

117 mill (Culatti, Switzerland). The rotor speed was adjusted to 7 and a standard sieve of 1 mm mesh
118 size was employed. Color of untreated hemp (B1-B4) and treated hemp shiv (C1-C4) was
119 determined. Each sample was measured at least in triplicate. The maximum of standard deviation
120 associated with the mean of measured values are, respectively, 3% for L* values, 6% for a*
121 values and 5 % for b* values.

122 **2.2.4 Biochemical composition of hemp shiv**

123 Biochemical composition of plant samples (B1-B4), ash content, lignin, cellulose, hemicellulose
124 and soluble contents, were determined following the method given by Van Soest method (NF
125 V18-122; Viel et al., 2018; Carrier et al., 2011) employing an adapted machine (FibercTR 8000,
126 Foss, Denmark). To carry out this measurement, all samples were previously dried until constant
127 weight at 40°C and then milled with the procedure described in section 2.2.3. All measurements
128 were carried out at least in triplicate.

129 **2.2.5 Vicat test**

130 The setting time of mortars was determined according to NF EN 196-3 using a manual Vicat
131 apparatus at room temperature. The shiv were ground to 2mm in order to make sure that the
132 aggregate will not interfere with the penetration of the Vicat needle. Thirteen samples were
133 prepared for the Vicat test, and the detail of the tested samples are given in Tab. 1. After
134 preliminary tests, it was found that when the water to binder ratio was 0.6 (e.g., water = 120g,
135 binder = 200g), the mortar had the best workability. Empirical observations indicated that water
136 treatment could effectively eliminate soluble components; therefore 6g of hemp shiv without
137 water treatment (i.e., shiv B in Fig. 1) and 120g of leachate (i.e., leachate D in Fig. 1)
138 theoretically contained the same quantity of soluble components. In addition, for each sample
139 shown in Tab. 1, a measure of penetration (at a random point) was made every 30 minutes by

140 recording the penetration depth of the needle into the paste. The Vicat test was repeated a total of
 141 three times, and the experimental results were the average value of these three repetitions.

142 **Table 1** Details of the tested samples. (B, C, and D correspond to the symbols in Fig. 1)

Symbol	Brief Introduction	Binder (g)	Shiv (g)	Water or Leachate* (g)
R	Reference (100% binder)	200	0	120
B1	Hemp shiv 1	194	6	120
B2	Hemp shiv 2	194	6	120
B3	Hemp shiv 3	194	6	120
B4	Hemp shiv 4	194	6	120
C1	Treated shiv 1	194	6	120
C2	Treated shiv 2	194	6	120
C3	Treated shiv 3	194	6	120
C4	Treated shiv 4	194	6	120
D1	Leachate 1	200	0	120*
D2	Leachate 2	200	0	120*
D3	Leachate 3	200	0	120*
D4	Leachate 4	200	0	120*

143

144 2.2.6 Thermogravimetric analysis

145 The thermogravimetric analysis (TGA) can be used to determine the $\text{Ca}(\text{OH})_2$ and CaCO_3 content
 146 of the sample. The aim of this experiment is to evaluate the long-term influence of hemp shiv
 147 leachate (i.e., D1-D4 in Tab. 1) on the carbonation process. Five samples (i.e., R, D1, D2, D3,
 148 and D4 in Tab. 1) were prepared at the same time and stored indoors under controlled conditions
 149 of temperature ($20 \pm 2^\circ\text{C}$) and relative humidity ($50 \pm 5\%$). For each sampling time (1 hour, 3 hours,
 150 7 hours, 1 day, 3 days, 7 days, 14 days, 28 days), 15g of the sample was gathered and stored in
 151 three sealed plastic tubes. Since the TGA test usually takes a long time (i.e., 2 hours for each
 152 sample), it was not possible to test all the samples at each sampling time. The sealed plastic tubes
 153 were soaked in liquid nitrogen (-196°C) for 30 seconds then stored in a -81°C freezer. This
 154 process was proved to be able to inhibit and even stop the hydration and carbonation reaction of
 155 the sample (Diquélou et al., 2015).

156 TGA analysis was carried out with the TG 209 F1 Iris Libra thermogravimetric analyzer
157 (produced by NETZSCH company). All experiments were conducted at temperature ranging from
158 25°C to 800°C with a heating rate of 10 °C/min under argon flow. Fig. 3 shows two examples of
159 the TGA curve. It is clear that sample weight changes occur in three areas, i.e., I, II, III in Fig. 3.

160 *Location of Figure 3*

161 Weight loss from 25°C to 380°C is mainly due to the loss of water from the pore and some
162 hydrate products (e.g., calcium silicate hydrate). While the reduction in weight from 380°C to
163 510°C and 510°C to 800°C are due to the decomposition of Ca(OH)₂ and CaCO₃ (Diquélou et al.,
164 2015), respectively. According to Fig. 3, it is observed that when the sampling time is 28 days,
165 the carbonation level of the sample prepared with leachate D3 is significantly lower than that of
166 the reference. This phenomenon will be analyzed in section 3.2.

167 The dry weight of Ca(OH)₂ and CaCO₃ (wt%) was calculated according to Eq. 1 and Eq. 2,
168 respectively, where LCO₂ represents the weight loss of CO₂ between 510°C and 800°C. LH₂O
169 and LH₂O' are the weight losses of water taking place between 25°C - 380°C and 380°C - 510°C.

170
$$Ca(OH)_2(wt\%) = LH_2O'(wt\%) \times \frac{MW(Ca(OH)_2)}{MW(H_2O)} \times \frac{1}{1 - LH_2O(wt\%)} \quad (Eq. 1)$$

171
$$CaCO_3(wt\%) = LCO_2(wt\%) \times \frac{MW(CaCO_3)}{MW(CO_2)} \times \frac{1}{1 - LH_2O(wt\%)} \quad (Eq. 2)$$

172 Here, MW is the abbreviation used for molecular weight, e.g., MW(CaCO₃) and MW(Ca(OH)₂)
173 represent the molecular weights of CaCO₃ and Ca(OH)₂, respectively i.e., 100.087g/mol and
174 74.093g/mol.

175

176

177 **3. Results and discussion**

178 **3.1 Setting time analysis**

179 The effect of hemp shiv and its leachate on the setting time of lime-based binders is shown in Fig.
180 4. The setting time of LHC using the hemp shiv without treatment is presented in Fig. 4a. Among
181 them, B3 and B4 had obvious delay effects on the setting. The delay was considerable, even
182 though the shiv dosage was significantly lower than that in a conventional LHC. Fig. 4b depicts
183 the setting time of the LHC using hemp shiv with water treatment and shows that after 24 hours
184 of water treatment, hemp shiv can significantly reduce the setting time. It is worth noting that all
185 treated hemp shiv accelerates the setting of LHC. Fig 4c describes the setting time of the LHC
186 using hemp shiv leachate and some of the leachate (e.g., D1, D2 in Fig. 4c) accelerates the setting
187 too. The mechanism of the accelerating effect was not studied in this work, which needs further
188 investigation on the chemical reaction of carbonation and hydration. The trends of the curves in
189 Fig 4a are similar to that of Fig 4c. The similarity of results between Fig. 4a and Fig. 4c indicate
190 that the retarding effect is mainly caused by the soluble components from hemp shiv (the leachate
191 contains mainly the soluble components like sugar and organic acids). The overlay of curves C1,
192 C2 and C3 are noticed and the shift of curve C4 implies that all soluble components from hemp
193 shiv B4 were not solubilized, and more than 24h of water treatment would have been required.

194 *Location of Figure 4*

195 It was found that there is a linear relation between hemp color and the retting degree, more the
196 hemp is rotten, the darker will be the color (Martin et al., 2013) for hemp shiv originating from
197 the same production batch. In this study, 4 different hemp shiv resulted from 4 production
198 batches. So, the prediction of the setting time of LHC by color analysis was not easy. However,
199 through visual observation, it was noticed that B4 is greener than other hemp shiv, and its LHC
200 has the longest setting time. In addition, no difference between untreated hemp shiv (B) and

201 treated hemp shiv (C) was visible whereas a difference in setting time was observed. Color
202 analysis was performed on powders of untreated hemp shiv (B1-B4 in Fig 5) and treated hemp
203 shiv (C1-C4 in Fig 5), as shown by results given in Fig. 5.

204 *Location of Figure 5*

205 The luminance (L) is a parameter which can vary from 0 to 100 and define respectively the
206 whiteness and the brightness. The mean for our L* values in Fig. 5 was 75. Martin et al. (2013)
207 observed a decrease of L* values from 70 to 50 progressively with the retting duration in case of
208 flax fibers. As all the values observed in our results were higher, it can be inferred that used hemp
209 shiv are probably all low retted. L*a*b* values were very similar for each hemp shiv, untreated or
210 treated, which supports our visual observation. However, values *b always decrease from B to C
211 samples, particularly for hemp shiv 3 and 4, from about 18 to 15. A decrease of parameter b
212 suggests an impact of treatment on color hemp and is an indicator of retting degree, as identified
213 by Martin et al. (2013) with flax fibers where a decrease of parameter b from 25 to 13 was
214 observed in 20 days of retting. The retting is a degradation of pectin through enzymes actions
215 produced by fungi (Meijer et al.,1995). The change of parameter b* between untreated and
216 treated hemp shiv suggests that hemp shiv 3 and 4 are less retted than hemp shiv 1 and 2. The
217 water treatment normally simulates the retting and is also involved in the release of pectin.
218 Investigations were also carried out to characterize hemp shiv for biochemical composition and
219 results are presented in Fig 6.

220 *Location of Figure 6*

221 Soluble fraction, hemicellulose, cellulose and lignin contents varied from 5.5 to 19,7 %, 16.2 to
222 20.7%, 53.9 and 62.4%, 9.4 to 15.4%, respectively. Which correspond to previous literature
223 studies (Diquélou et al., 2015; Viel et al., 2018). Hemp shiv B4 demonstrated a slightly different
224 composition from the others with the highest fraction of soluble compounds. The composition of

225 this fraction includes different soluble compounds such as fat, wax, pectin, proteins and
226 polysaccharides (Viel et al., 2018). So, hemp shiv B4, comprising the higher fraction of pectin is
227 probably the less retted.

228 Due to cost and time consumption aspects, spectrophotometry and Van Soest methods are not
229 considered to be feasible for application at industrial scale. It is necessary to find a simple and
230 sensitive method to predict the setting time and the compatibility of LHC, therefore we studied
231 the leachate using pH and conductivity analysis.

232 The hemp shiv leachate (i.e., D1-D4 in Tab. 1) is shown in Fig. 7. It was found that the color of
233 leachate D4 was significantly darker than the others. For leachate D1-D3, even though the color
234 of hemp shiv (i.e., B1-B3 in Fig. 1) is different, their leachate appears identical. For further
235 evaluation of the leachate, pH and conductivity analysis were performed for D1-D4 leachate. The
236 results of the pH and conductivity analysis are shown in Tab. 2.

237 *Location of Figure 6*

238 **Table 2** pH and conductivity of the leachate D1-D4. (The weight loss is the weight reduction of
239 10g hemp shiv after water treatment)

Sample	pH	Conductivity (mS/cm)	Weight loss (g)
Water	6.946	0.003	-
D1	6.797	1.472	0.77
D2	7.673	0.949	0.43
D3	7.127	1.853	1.25
D4	5.49	3.54	1.41

240

241 It can be seen from Table. 2 that D3 and D4 present the highest weight loss and conductivity
242 values. The leachate concentration suggests a mass concentration based on the difference of hemp
243 masses before and after water treatment. The weight loss of the hemp shiv has a linear correlation

244 with the concentration of leachate substance. It was found that the conductivity and the loss
245 roughly correspond to the setting time (Fig. 4c), higher the weight loss (or conductivity) longer
246 the setting time. Usually, farmers control the duration of field retting based on the color changes
247 and their experiences. This experiment result indicated that the weight loss could be a helpful
248 indicator for the industry to predict the setting time of LHC and test the retting degree. To reveal
249 the mechanism of the setting retardation, the leachate was analyzed by infrared spectrum.

250 As the concentration of the leachate was too small to be tested, it was necessary to concentrate the
251 soluble component, thus the freeze-drying method was used to get the components in the
252 leachate. The dehydrated soluble components are shown in Fig. 8. Colors and textures of
253 dehydrated soluble components are different, suggesting a variability in their content and
254 chemical composition.

255 *Location of Figure 8*

256 The freeze-drying substances of the leachate (Fig. 8) were analyzed by FT-IR spectrum (Fig. 9).

257 *Location of Figure 9*

258 The most diagnostic FT-IR bands were 1050 cm^{-1} (C-O stretch), 1404 cm^{-1} (O-H), and 1558 cm^{-1}
259 (in-plane NH_2 scissoring), the first two bands correspond to the carbohydrate (Dorado et al.,
260 2001) whilst the second corresponds to amides. The intensity of band 1050 cm^{-1} had a positive
261 correlation with the field retting duration (Walker et al., 2014), which indicated that the sample
262 having low retting degree (B3 in Fig. 1) comprised more carbohydrates. The intensity of band
263 1558 cm^{-1} of D4 spectrum meant hemp shiv B4 contained amide functions. The amides in plants
264 are mainly derived from asparagine and glutamine, which are formed through photosynthesis in
265 plants. Other main sources of these amides are plant proteins and some co-enzymes.

266 It is a well-known fact that saccharides could delay the setting time (Wang et al., 2019) of cement
267 and that hemp leachates were rich in some monomeric sugars (e.g., galactose, glucose, fructose)
268 (Tronet et al., 2016; Kochova et al., 2017; Delannoy et al., 2020), which could explain the
269 retarding effect of hemp shiv B3, B4 and its leachate D3, D4 (Fig. 4). However, the hemp shiv B4
270 and its leachate D4 obviously contain more soluble fraction than other hemp shiv samples, as
271 shown in Fig. 6 and Fig. 7. Therefore, the 24h water treatment may not be long enough, resulting
272 in a longer setting time for the treated hemp shiv C4 than other hemp shiv samples (Fig. 4b). The
273 high intensity of spectrum band 1050 cm^{-1} and the low pH (Tab. 2) indicated that the leachate D4
274 was rich in carboxylate group (COOH) originating from galacturonic acids, which in turn are
275 probably derived from pectin. Kochova et al. (2017) proved that the pH of the leachate could be
276 used as an indicator of the cement-plant aggregates compatibility, and acid admixture might slow
277 down the cement setting (Uchikawa et al., 1995; Gori et al., 2011). Bruere (1966) and Smith et al.
278 (2011) found that the set-retarding saccharides (e.g., maltose, lactose, glucose) either contain the
279 OH-C-C=O group or can be converted by dilute alkali into saccharides acids containing this
280 group. The oxygen molecules of this particular group can approach each other and adsorb on the
281 surface of $\text{Ca}(\text{OH})_2$ or cement particles by a chelation reaction (Young 1972; Juenger and
282 Jennings, 2002; Thomas et al., 2009).

283 The hemp leachate influenced not only the setting time of the lime-based matrix, but section 3.2
284 indicated that the carbonation reaction was also affected by the leachate. It can be supposed that
285 not only the cement particle, but the calcium hydroxide particle was chelated or complexed with
286 organic components. It is well known that popular cement retarders such as sodium gluconate and
287 lignosulfonate can form complexes with Ca^{2+} , reduce the concentration of calcium ions in the
288 solution, and the presence of these complexes on the surface of the cement particles inhibit
289 cement hydration. Since there is a large amount of $\text{Ca}(\text{OH})_2$ in the lime-based matrix, there is no
290 shortage of Ca^{2+} ions, so a more reasonable explanation is the chelate formed by the organic

291 matter (i.e., sugar and amide) and Ca^{2+} precipitates and adheres to the cement and calcium
292 hydroxide particle.

293 Hydroxycarboxylic acid, provided by the leachate solution has both carboxylic and hydroxyl
294 groups. Carboxylic group COO^- adsorbs on the surface of mineral particles through forming a
295 complex with Ca^{2+} by electrostatic interaction. However, high COO^- content might lead to higher
296 water bleeding and a long setting time of the concrete (Young 1972; Sha et al., 2020). Hydroxyl
297 group would interact with surface Ca^{2+} ions, while the latter could bond simultaneously to
298 adjacent O^{2-} ions (Young 1972). In addition, Ca^{2+} forming ligands with nitrogen atoms in amide
299 structure, decreases the concentration of available Ca^{2+} ions (Liu et al., 2014). Thus, the
300 formation of calcium hydroxide and C-S-H gel were delayed, and the good flowability of cement
301 pastes maintained a longer time (Sha et al., 2020). Diquélou et al. (2015) demonstrated that strong
302 retarding agents and a reduction in the number of hydrates (C-S-H and portlandite) were
303 observed. This considerable modification of the setting and hardening process is further
304 illustrated with the loss of mechanical properties.

305 The above explanation interpreted the mechanism that the less rotten hemp shiv delays the setting
306 of LHC. Both the saccharides and organic acids from hemp shiv might have delayed the setting
307 and decreased the compatibility of LHC. Experiments showed that 24 hours of water treatment
308 could effectively eliminate these substances. However, it was not clear through which mechanism
309 the hemp leachate (i.e., hemp leachate D1 and D2 in Fig. 4) accelerated the setting time. So, the
310 long-term influence of the hemp shiv leachate on the binder was explored in the following section
311 [3.2](#).

312 **3.2 Carbonation reaction**

313 The lime carbonation reaction is a chemical reaction in which calcium hydroxide ($\text{Ca}(\text{OH})_2$)
314 reacts with carbon dioxide (CO_2) and forms insoluble calcium carbonate (CaCO_3). The

315 mechanism and the kinetics of the carbonation depend strongly on the CO₂ concentration and the
316 moisture (Despotou et al., 2016). Fig. 10 (a and b) showed the results of thermogravimetric
317 analysis (the calculation method is in 2.2.6), which highlight the change of CaCO₃ and Ca(OH)₂
318 contents in the presence of hemp shiv leachate at different sampling times (1h, 3h, 7h, 1d, 3d, 7d,
319 14d, 28d and 90d).

320 *Location of Figure 10*

321 It was found that the contents of CaCO₃ and Ca(OH)₂ were negatively correlated, but the change
322 of Ca(OH)₂ content was relatively complicated. The main reason is that the content of calcium
323 hydroxides was affected by carbonation reaction, cement hydration and pozzolanic reaction. Fig.
324 10 depicted that during the first 7 hours, the Ca(OH)₂ content of D4 was lower than others, which
325 was mainly because of the low pH of leachate D4. In the first 7 hours, the sample D1 and D2
326 (Fig. 4c) almost finished the setting while their CaCO₃ content had no apparent difference with
327 other samples. This phenomenon indicated that the carbonation reaction had no significant effect
328 on the setting time (in fact the carbonation reaction is a long-term reaction which takes several
329 months). It was the hydration of the cement that determines the setting time.

330 As far as the long-term carbonation reaction is concerned, it was observed that from the seventh
331 day that the CaCO₃ content of D3 and D4 were significantly lower than that of other samples. It
332 was recognized that leachate D3 and D4 have higher mass loss and conductivity (Tab. 2), which
333 revealed that the conductivity of the leachate and weight loss of the hemp could be an indicator to
334 predict the carbonation rate of the LHC. We proposed the hypothesis that setting retarder
335 (leachate D3 and D4 in Fig. 4c) tends to have lower carbonation levels, which mean that the
336 hemp shiv which retarded the setting could prevent the carbonation reaction and even influence
337 the mechanical performance.

338 **4. Conclusion**

339 This research evaluated the influence of different hemp shiv on the setting time and the
340 carbonation of lime-based binder. Empirical observations and experimental results showed that
341 the low rotten shiv tend to have compatibility problems with the binder and prolong the setting
342 time. The Vicat test proved that it was due to the soluble components (e.g., organic acids, simple
343 sugars, proteins) of the shiv which influenced the hydration and carbonation reactions. In general,
344 the color was considered an effective way to assess the degree of retting, but the present study
345 revealed that the color was not linearly related to the setting time of LHC. In this research, we
346 found that water treatment can effectively remove the retarding agent. These findings indicated
347 the potential use of water treatment to improve the compatibility between hemp shiv and lime
348 matrix. The weight loss of hemp shiv after water treatment can be a useful indicator to evaluate
349 the retting degree and predict the setting delay. Considering the pH and conductivity of leachate,
350 the prediction can be more accurate. However, there are still many phenomena (e.g., some
351 leachates accelerate solidification and hardening) and mechanisms (e.g., mechanism of the effect
352 of leachate on carbonation) that cannot be explained now, as this requires further investigation.

353 Benhelal E., Zahedi G., Shamsaei E., Bahadori A., 2013. Global strategies and potentials to curb CO2
354 emissions in cement industry. *J Clean Prod* 51, 142-161.

355 Bilba K., Arsène M-A., Ouensanga A., 2003. Sugar cane bagasse fibre reinforced cement composites. Part
356 I. Influence of the botanical components of bagasse on the setting of bagasse/cement composite. *Cement*
357 *Concrete Comp* 25, 91-96.

358 Bruere G-M., 1966. Set-retarding effects of sugars in Portland cement pastes. *Nature* 212, 502-503.

359 Carrier M., Loppinet-Serani A., Denux D., Lasnier J-M., Ham-Pichavant F., Cansell F., Aymonier C.,
360 2011. Thermogravimetric analysis as a new method to determine the lignocellulosic composition of
361 biomass. *Biomass Bioenerg* 35, 298-307.

362 [Delannoy G., Marceau S., Gle P., Gourlay E., Guéguen-Minerbe M., Diafi D., Amziane S., Farcas F., 2020.](#)
363 [Impact of hemp shiv extractives on hydration of Portland cement. *Construction and Building Materials*,](#)
364 [244, 118300.](#)

365 Despotou E., Shtiza A., Schlegel T., Verhelst F., 2016. Literature study on the rate and mechanism of
366 carbonation of lime in mortars/Literaturstudie über Mechanismus und Grad der Karbonatisierung von
367 Kalkhydrat im Mörtel. *Mauerwerk* 20, 124-137.

368 Diquélou Y., Gourlay E., Arnaud L., Kurek B., 2015. Impact of hemp shiv on cement setting and
369 hardening: Influence of the extracted components from the aggregates and study of the interfaces with the
370 inorganic matrix. *Cement Concrete Comp* 55, 112-121.

371 Dorado J., Almendros G., Field J A., Sierra-Alvarez R., 2001. Infrared spectroscopy analysis of hemp
372 (*Cannabis sativa*) after selective delignification by *Bjerkandera* sp. at different nitrogen levels. *Enzyme*
373 *Microb Tech* 28(6), 550-559.

374 Elfordy S., Lucas F., Tancret F., Scudeller L., Goudet L., 2008. Mechanical and thermal properties of lime
375 and hemp concrete (“hemcrete”) manufactured by a projection process. *Constr Build Mater* 22, 2116-
376 2123.

377 Gori M., Bergfeldt B., Pfrang-Stotz G., Reichelt J., Sirini P., 2011. Effect of short-term natural weathering
378 on MSWI and wood waste bottom ash leaching behaviour. *J Hazard Mater* 189, 435-443.

379 Hirst E., Walker P., Paine K., Yates T., 2010. Characterisation of low density hemp-lime composite
380 building materials under compression loading. In: *The 2nd international conference on sustainable*
381 *construction materials and technologies*, Italy, 1395-1406.

382 Ip K., Miller A., 2012. Life cycle greenhouse gas emissions of hemp–lime wall constructions in the UK.
383 *Resour Conserv Recy* 69, 1-9.

384 Juenger M-C-G., Jennings H-M., 2002. New insights into the effects of sugar on the hydration and
385 microstructure of cement pastes. *Cement Con Res* 32, 393-399.

386 Khazma M., Goullieux A., Dheilley R-M., Quéneudec M., 2012. Coating of a lignocellulosic aggregate with
387 pectin/polyethylenimin mixtures: Effects on flax shive and cement-shive composite properties. *Cement*
388 *Concrete Comp* 34, 223-230.

389 Kochova K., Schollbach K., Gauvin F., Brouwers H-J-H., 2017. Effect of saccharides on the hydration of
390 ordinary Portland cement. *Constr Build Mater* 150, 268-275.

391 Li Y., Pickering K-L., Farrell R-L., 2009. Analysis of green hemp fibre reinforced composites using bag
392 retting and white rot fungal treatments. *Ind Crop Prod* 29, 420-426.

393 Liu X., Wang Z., Zhu J., Zheng Y., Cui S., Lan M., Li H., 2014. Synthesis, characterization and
394 performance of a polycarboxylate superplasticizer with amide structure. *Colloids Surface B* 448, 119-129.

395 Martin N., Mouret N., Davies P., Baley C., 2013. Influence of the degree of retting of flax fibers on the
396 tensile properties of single fibers and short fiber/polypropylene composites. *Ind Crop Prod* 49, 755-767.

397 Mazian B., Bergeret A., Benezet J-C., Malhautier L., 2018. Influence of field retting duration on the
398 biochemical, microstructural, thermal and mechanical properties of hemp fibres harvested at the beginning
399 of flowering. *Ind Crop Prod* 116, 170-181.

400 Meijer W-J-M., Vertregt N., Rutgers B., Van de Waart M., 1995. The pectin content as a measure of the
401 retting and rettability of flax. *Ind Crop Prod* 4, 273-284.

402 **NF EN 196-3. 2017. Méthodes d'essais des ciments - Partie 3 : détermination du temps de prise et de la**
403 **stabilité. AFNOR.**

404 **NF V18-122, 2013. Aliments des animaux-Détermination séquentielle des constituants pariétaux-Méthode**
405 **par traitement aux détergents neutre et acide et à l'acide sulfurique. AFNOR.**

406 Prétot S., Collet F., Garnier C., 2014. Life cycle assessment of a hemp concrete wall: Impact of thickness
407 and coating. *Build Environ* 72, 223-231.

408 Sáez-Pérez M-P., Brümmer M., Durán-Suárez J-A., 2020. A review of the factors affecting the properties
409 and performance of hemp aggregate concretes. *J Build Eng* 31, 101323.

410 Sanjay M-R., Madhu P., Jawaid M., Senthamarai kannan P., Senthil S., Pradeep S., 2018. Characterization
411 and properties of natural fiber polymer composites: A comprehensive review. *J Clean Prod* 172, 566-581.

412 Sedan D., Pagnoux C., Smith A., Chotard T., 2008. Mechanical properties of hemp fibre reinforced cement:
413 Influence of the fibre/matrix interaction. *J Eur Ceram Soc* 28, 183-192.

414 Sha S., Wang M., Shi C., Xiao Y., 2020. Influence of the structures of polycarboxylate superplasticizer on
415 its performance in cement-based materials-A review. *Constr Build Mater* 233, 117257

416 Smith B-J., Rawal A., Funkhouser G-P., Roberts L-R., Gupta V., Israelachvili J-N., Chmelka B-F., 2011.
417 Origins of saccharide-dependent hydration at aluminate, silicate, and aluminosilicate surfaces. *P Natl Acad*
418 *Sci Usa* 108, 8949-8954.

419 Thomas J-J., Jennings H-M., Chen J-J., 2009. Influence of nucleation seeding on the hydration mechanisms
420 of tricalcium silicate and cement. *J Phys Chem C* 113, 4327-4334.

421 Tronet P., Lecompte T., Picandet V., Baley C., 2016. Study of lime hemp concrete (LHC)–Mix design,
422 casting process and mechanical behaviour. *Cement Concrete Comp* 67, 60-72.
423 <https://doi.org/10.1016/j.cemconcomp.2015.12.004>

424 Uchikawa H., Sawaki D., Hanehara S., 1995. Influence of kind and added timing of organic admixture on
425 the composition, structure and property of fresh cement paste. *Cement Concrete Res* 25, 353-364.

426 Viel, M., Collet, F., Lanos, C., 2018. Chemical and multi-physical characterization of agro-resources' by-
427 product as a possible raw building material. *Ind Crop Prod* 120, 214-237.

428 Walker R., Pavía S., 2014. Effect of hemp's soluble components on the physical properties of hemp
429 concrete. *J Mater Sci Res* 3, 12-23.

430 Walker R., Pavia S., Mitchell R., 2014. Mechanical properties and durability of hemp-lime concretes.
431 *Constr Build Mater* 61, 340-348.

432 Wang L., Lenormand H., Zmamou H., Leblanc N., 2019. Effect of soluble components from plant
433 aggregates on the setting of the lime-based binder. *J Renew Mater* 7, 903-913.

434 Worrell E., Price L., Martin N., 2001. Carbon dioxide emissions from the global cement industry. *Annu*
435 *Rev Energ Env* 26, 303-329.

436 Young J-F., 1972. A review of the mechanisms of set-retardation in Portland cement pastes containing
437 organic admixtures. *Cement Concrete Res* 2, 415-433.

438 **Figure 1** Schematic diagram of the material preparation process

439 **Figure 2** Photographs of the tested hemp shiv before and after water treatment. B1-B4: hemp shiv
440 before water treatment; C1-C4: hemp shiv after water treatment

441 **Figure 3** Thermogravimetric curves of samples D3 and R at 28 days

442 **Figure 4** Setting time of lime-based binder with the addition of (a): hemp shiv without water
443 treatment; (b): hemp shiv after water treatment; (c): hemp shiv leachate. (The symbols B1-B4,
444 C1-C4, and D1-D4 correspond to the symbols shown in Tab. 1)

445 **Figure 5** Color analysis of untreated hemp shiv (B1-B4) and treated hemp shiv (C1-C4)

446 **Figure 6** Biochemical composition of 4 different hemp shiv

447 **Figure 7** Leachates D1-D4 of the hemp shiv

448 **Figure 8** Soluble components in leachates after freeze-drying

449 **Figure 9** The infrared spectrum of the leachates after freeze drying.

450 **Figure 10** (a) The change in CaCO_3 content of the lime-based binder in the presence of hemp
451 leachate D1-D4. (b) The change in Ca(OH)_2 content of lime-based binder in the presence of hemp
452 leachate.

453 **Table 1** Details of the tested samples. (B, C, and D correspond to the symbols in Fig. 1)

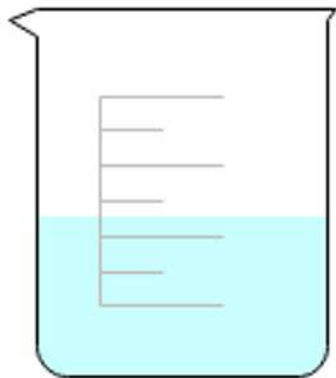
454 **Table 2** pH and conductivity of the leachate D1-D4. (The weight loss is the weight reduction of

455 10g hemp shiv after water treatment)

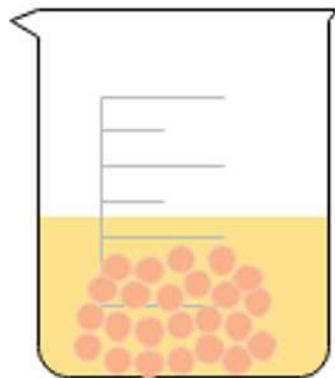
B: 10g hemp shiv



+



A: 200g water



210g Mixture.
20°C, 24h

Filtration

Drying
60°C, 24 h

C: ≈ 9 g treated hemp
shiv



D: ≈ 201 g
leachate

B1

B2

B3

B4

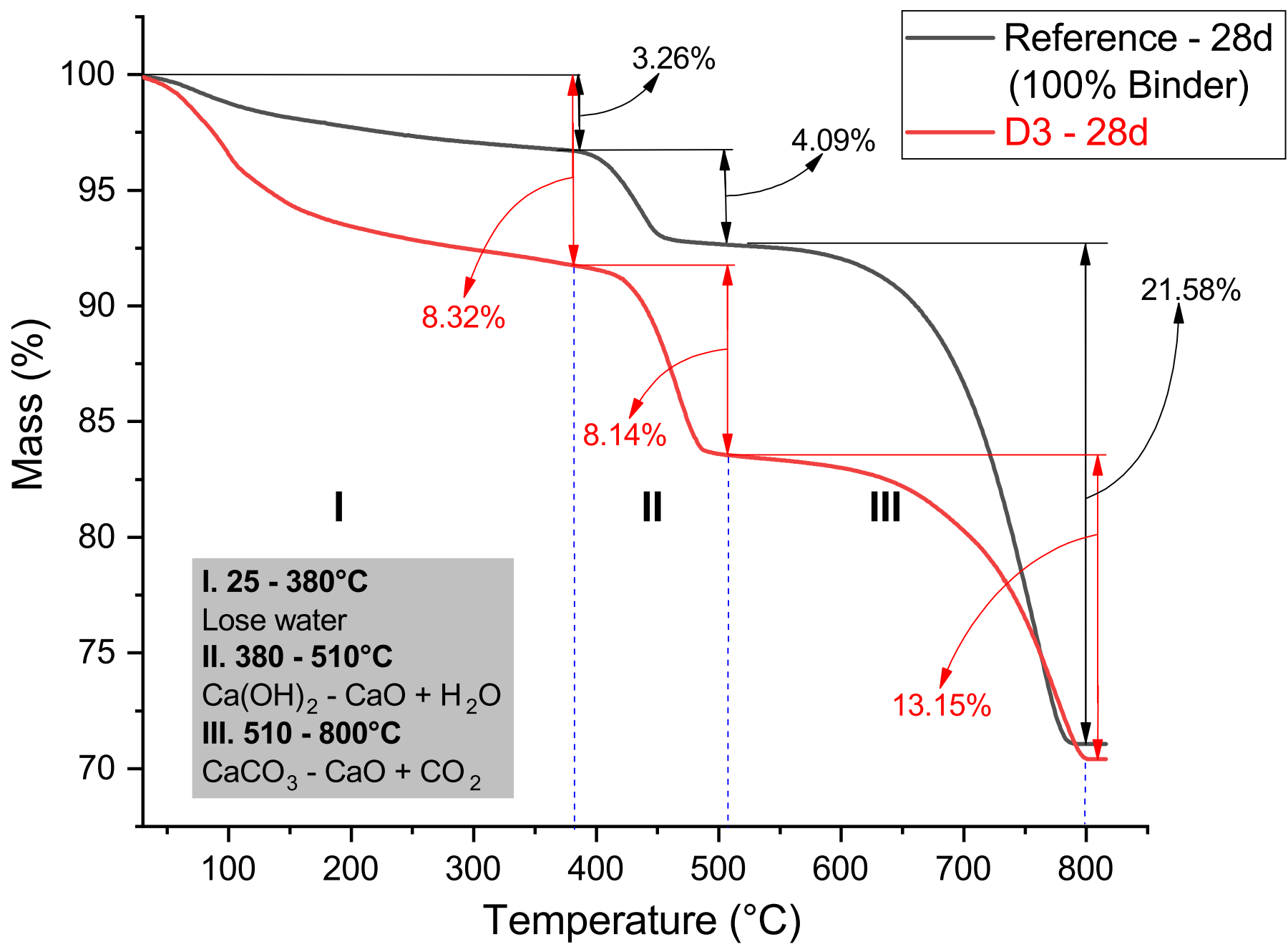
C1

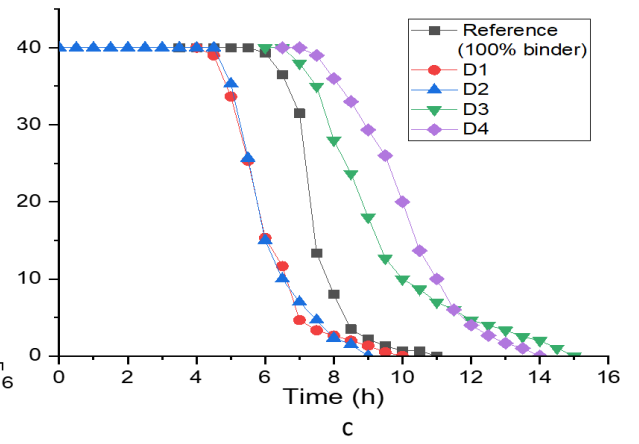
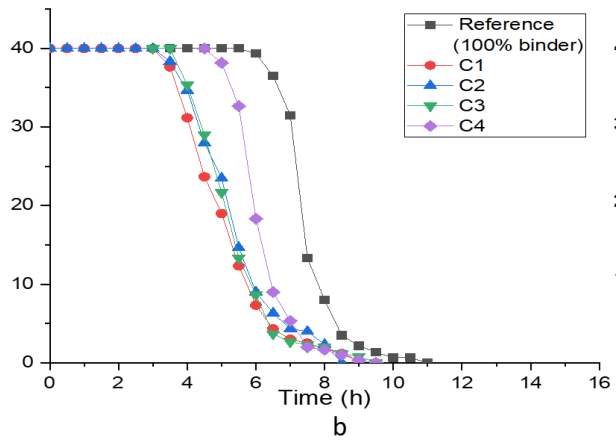
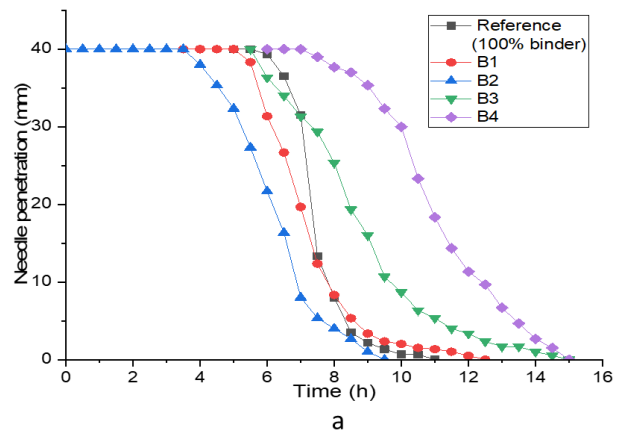
C2

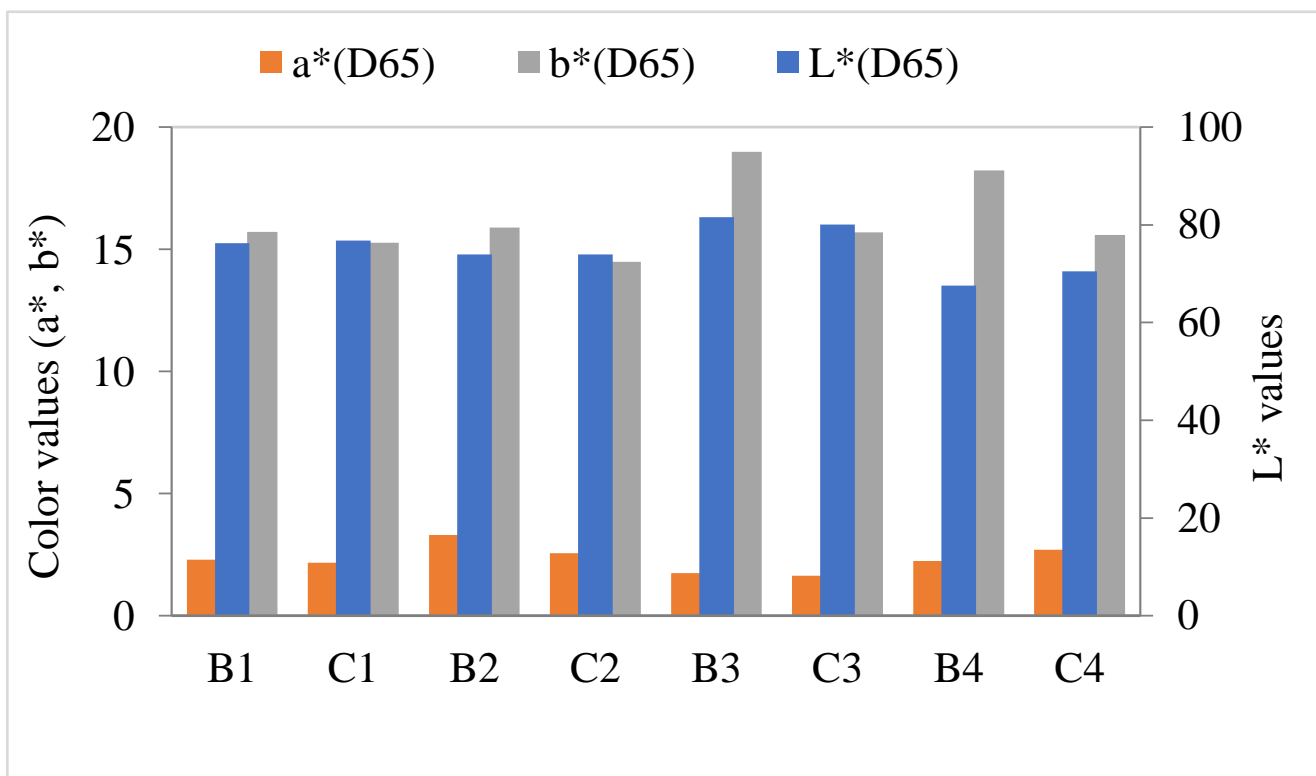
C3

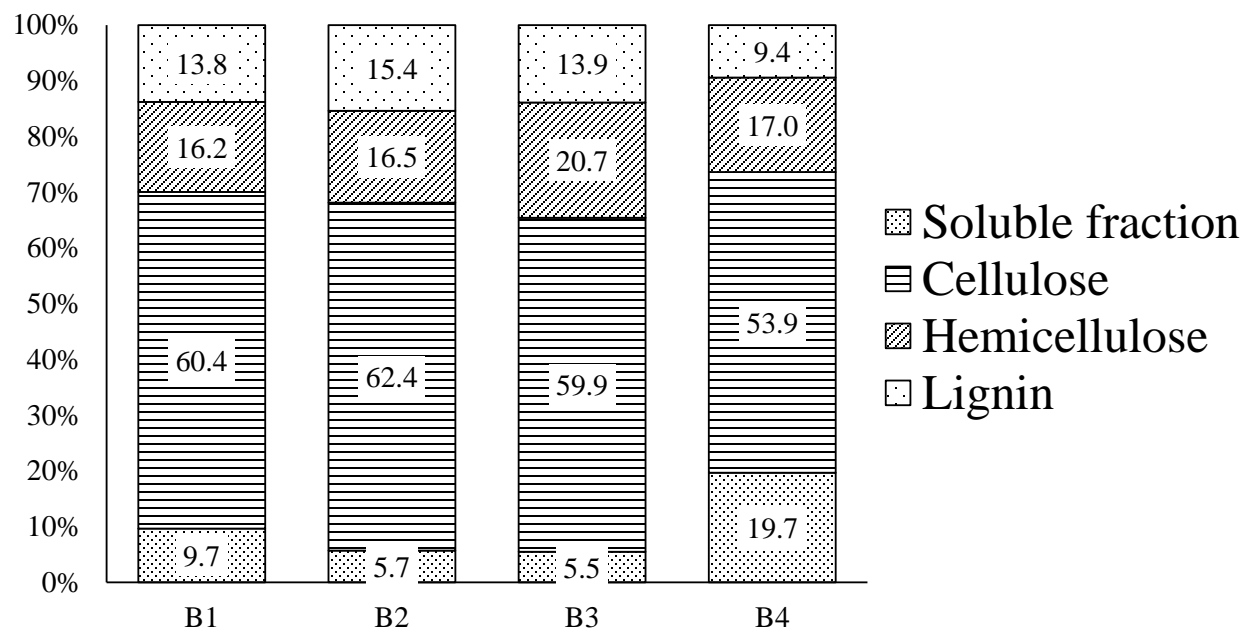
C4











D1

D2

D3

D4

H₂O

